Measuring the global and directed propagation of several quality indicators in the optimal design of parallel robots through the evaluation of Lipschitz and GTI indices

Le Huu Hung[1], Pham Thanh Long[2], Nguyen Thi Trang Nhung[2*]

[1]College of Technology and Trade, Bach Quang, Thai Nguyen, Vietnam;
[2]Thai Nguyen University of Technology, 3-2 Street, Tich Luong, Thai Nguyen, Vietnam.
[*]Corresponding author: trangnhung.dhktcn@tnut.edu.vn
Received 12 Jan. 2026; Revised 15 Mar. 2026; Accepted 15 Jun. 2026; Published 25 Jun. 2026.
DOI: https://doi.org/10.54939/1859-1043.j.mst.112.2026.11-19

ABSTRACT

In the optimal design of multi-objective parallel robots, transmission ratios such as n_{vmin} and n_{pmin} are used to evaluate the extent to which velocity and force propagate from the joint space (q) to the robot's work space (x). Two pieces of information need to be measured in this evaluation: the degree of overlap between the drive and the actuator, and the amplification/attenuation of the drive when it becomes the actuator. Two methods are used to evaluate these factors: assessing the propagation across the entire space using the Lipschitz coefficient and evaluating in a specific direction of interest using the GTI (Geometric Transmission Index). In the improved Atlas algorithm proposed by the author, the Pareto boundary is defined as the intersection of convergent directional cones based on the propagation guidance atlases of the aforementioned design parameters. This paper introduces a method for evaluating these coefficients in the discrete design domain ri to automate the process of determining the Pareto boundary, thereby providing a basis for automating the entire design.

Keywords: Jacobian; GTI; Spread; Lipschitz; Global.

1. INTRODUCTION

The optimal design of parallel robots has drawn considerable attention for its high stiffness, large load capacity, and high positioning accuracy. Performance indices such as stiffness, dexterity, and transmission indices are widely used to evaluate motion/force transmission from joint space (q) to Cartesian space (x), and multi-objective optimization is increasingly applied to improve several criteria at once. However, most studies focus on optimal parameters while giving comparatively little attention to how performance indices propagate across the design space.

In the classical Atlas-based approach, the criteria $1/K$, n_{vmin}, and n_{pmin} act as three independent guiding channels that determine the Pareto frontier. These atlases map the transmission of force and velocity from (q) to (x); the directional alignment of actuation in (q) governs the amplification or sensitivity of the mapping into (x).

A parallel robot is considered optimally designed with respect to both criteria when it exhibits a favorable minimum velocity, meaning minimal velocity loss to sustain high productivity throughout the Cartesian workspace (x), and simultaneously possesses high stiffness, i.e., a strong capability to generate force in the workspace. To identify stable parameter regions with high convergence levels for these criteria, both directional and global performance indicator maps are of critical importance [1–4].

In existing studies, these performance measures are typically treated separately within single-objective optimization frameworks. The procedure involves tracking each signal from an arbitrary point on the corresponding atlas and moving along the associated directional cones where performance improves, until no further enhancement is possible. If an intersection region exists among the terminal directional cones, it defines a Pareto frontier, which constitutes the a posteriori

solution of the multi-objective optimal design problem. The principal limitation of this approach is that, when the atlases are defined over a continuous domain, they cannot be processed automatically; instead, subjective human interpretation is required to extract the Pareto frontier [5–7].

This paper introduces a method for quantifying these transmission performances in the form of global indices and directional indices, defined through the Lipschitz constant and the GTI coefficient over a discrete space. Superimposing numerical solutions on a discrete domain provides a pathway toward full automation of the optimal design of parallel mechanisms. Moreover, this structured dataset serves as essential input for training surrogate models when extending the framework to large-scale data-driven optimization [8–9]. Consequently, the measurement of transmission levels of performance indices in both scalar and directional forms plays a decisive role in the improved Atlas-based optimization algorithm.

2. GUIDING ROLE OF STRUCTURED DATA

2.1. Classical Atlas-based method [1-4]

Assume that the original multi-objective optimization problem is formulated as (1):

$$\begin{aligned} &\min f = [f_1, f_2, \ldots f_n] \\ &r \in B \end{aligned} \tag{1}$$

where B is the composite domain of design parameters r, and fi is the i-th optimal transmission performance index. All indices fi are constructed as atlases over the continuous domain r, as illustrated in Figure 1.

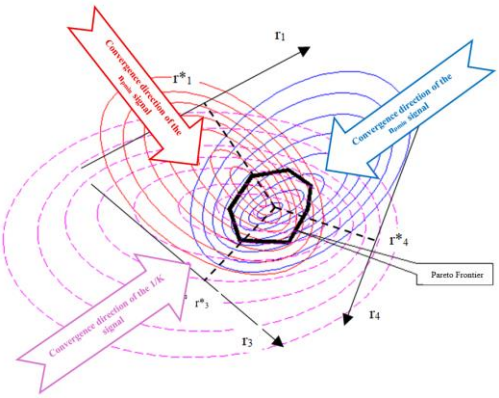

Figure 1. *Role of performance atlases in shaping the Pareto frontier.*

At any point, each atlas fi defines a cone of convergent directions along which the objective improves. If an intersection of these cones exists, it forms the set of non-dominated points — the Pareto frontier of the classical Atlas framework.

This approach is valued because it decomposes problem (1) into subproblems of the form:

$$\begin{aligned} &\min f_i \\ &r \in B \end{aligned} \tag{2}$$

Under this rationale, the essence of the Atlas-based approach lies in constructing the performance atlases f_i individually prior to aggregating them for the final decision-making stage. At this point, the problem reduces to the automation of the superposition process: instead of representing f_i over a continuous domain, as illustrated in Figure 1, they must be recomputed over a discrete domain.

2.2. Jacobian-based performance ratio indices

Robotics defines two spaces: the Cartesian workspace (x) and the joint space (q). Control

actions originate in (q) and are transmitted to (x). Forces, velocities, and errors follow the Jacobian mapping [10, 11], which can be expressed as in (3):

$$q' = J^{-1}.x' \tag{3}$$

Producing a Cartesian quantity x' at the end-effector requires a corresponding actuation q'; the normalized ratio q'/x' is the transmission ratio of that quantity, realized through the Jacobian matrix J.

If the desired Cartesian output is not aligned with x' but required along an observation direction h, only part of the work done by x' is useful. Premultiplying both sides of Equation (3) by h^T gives the useful work component:

$$h^T.q' = h^T.J^{-1}.x' \tag{4}$$

So the effective transmission level along h is the normalized projection of $(J^{-1}x')$ onto the direction h [10], as defined in Equation (5):

$$GTI(x', h) = \frac{\left|h^T.(J^{-1}x')\right|}{\|h\|.\left\|J^{-1}.x'\right\|} \tag{5}$$

The numerator of the GTI represents the useful component along the observation direction h, whereas its denominator corresponds to the total work expended. In other words, the GTI evaluates the transmission ratio along the observation direction h.

As defined in Equation (5), the GTI measures the degree of directional alignment between the cause $(J^{-1}x')$ and the effect h.

If the magnitude of $(J^{-1}x')$is normalized to unity, Equation (5) reduces to Equation (6):

$$GTI(x', h) = \frac{\left|h^T.(J^{-1}.x')\right|}{\|h\|.\left\|J^{-1}.x'\right\|_{\max}} \tag{6}$$

This dimensionless form also shows how the useful component's magnitude varies along h. GTI is maximal when the actuation direction aligns with h, and zero when the two are orthogonal.

Depending on the normalization adopted for the denominator in Equation (6), the GTI may also admit a second interpretation:

- Let the Lipschitz constant be denoted by L, representing the global bound of the transmission amplification in the mapping between spaces [5, 11], and define:

$$L = \max_{\|x'\|=1} \left\|J^{-1}.x'\right\| \tag{7}$$

That is, considering all directions of x' and taking the worst case, GTI then measures amplification over the entire space, in which case GTI assumes the nature of a Lipschitz constant.

2.3. Interpretation of transmission ratios based on the ellipsoidal transformation

The transmission behavior can also be interpreted through the ellipsoidal transformation of the Jacobian [10-11]. Assume a unit sphere in the Cartesian workspace x, with normalized force and velocity given by:

$$A = (J.J^T) = 1 \tag{8}$$

$$A = (J.J^T)^{-1} = 1 \tag{9}$$

From Equation (10) below, the eigenvalues and eigenvectors of A can be determined:

$$(A - \lambda.I)x = 0 \tag{10}$$

Excluding the trivial solution x = 0: if λ1 = λ2 = λ3, the mapped unit sphere remains a sphere; if λ1 = λ2 ≠ λ3, it becomes a spheroidal (axisymmetric) ellipsoid; if λ1 ≠ λ2 ≠ λ3, it becomes a general ellipsoid with principal semi-axes λ1, λ2, λ3 along eigenvectors x1, x2, x3, as illustrated in Figure 2.

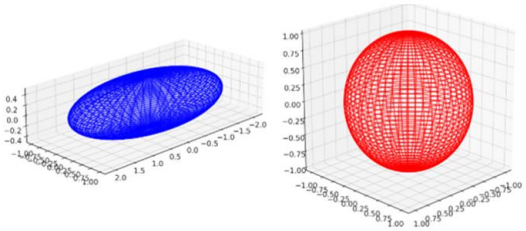

Figure 2. *Illustration of the mapping from a unit sphere in* (x) *to an ellipsoid in* (q).

At this stage, a new index, termed the Global Constraint Index (GCI), is introduced based on these semi-axes. It quantifies the worst-case transmission ratio over the entire space, as defined in Equation (11):

$$GCI = \frac{\|\lambda_{min}\|}{\|\lambda_{max}\|} \tag{11}$$

Where:

$$\|\lambda_{\max}\| = \max(\|\lambda_1\|, \|\lambda_2\|, \|\lambda_3\|);\ \|\lambda_{\min}\| = \min(\|\lambda_1\|, \|\lambda_2\|, \|\lambda_3\|) \tag{12}$$

Accordingly, on the ellipsoidal surface, the relationship among the performance measures GTI, GCI, and the Lipschitz constant can be established as expressed in Equation (13):

$$GCI \subset GTI \subset Lipschitz \tag{13}$$

At any point in q, the ellipsoid is the image of a unit sphere in x. A point on the ellipsoidal surface not coinciding with a principal axis gives a radius equal to the GTI along that direction; considering only the principal semi-axes gives the most extreme case — the GCI. Unlike GTI (evaluated in all directions), GCI is concerned solely with the worst case; both are defined on the same ellipsoidal surface and are thus special cases of one another (Equation 13). Collecting all extreme directions over the entire joint space q yields the Lipschitz constant.

Now, discretize the continuous design space li and parameter space ri of the classical Atlas approach, and define an axis-transformation relationship under the improved Atlas framework [8-9]:

$$r_i = R.x_i \tag{14}$$

where R is the axis-transformation matrix fixed by the arrangement of ri relative to the xyz frame. The spreading process over the discrete domain ri thereby becomes fully automated, as illustrated in Figure 3, rather than relying on subjective interpretation as in Figure 1.

No.	Coordinates	η_{pmin}	1/K	η_{vmin}	Total
1	$x_1y_1z_1$	0.55	0.62	0.34	1.96
2	$x_2y_2z_2$				-
3	$x_3y_3z_3$				-
4	$x_4y_4z_4$				-
5	$x_5y_5z_5$				-
6	$x_6y_6z_6$				$\sum$ max
7	$x_7y_7z_7$				$\sum$ max
…	…				-
…					-
…					-
n	$x_ny_nz_n$				-

Figure 3. *Propagation directions of GTI ratios in the Improved Atlas Framework.*

Weak signals appear in blue, increasing through yellow and pink to a maximum at red.

Convergence-direction information is preserved relative to the continuous-domain atlas of Figure 1, while the Pareto frontier is now obtained directly along the red rows (rows 6 and 7 in Figure 3).

3. ILLUSTRATION WITH A DELTA PARALLEL ROBOT

The Delta parallel robot is a widely applied industrial mechanism designed for high-speed, high-precision tasks in a compact workspace.

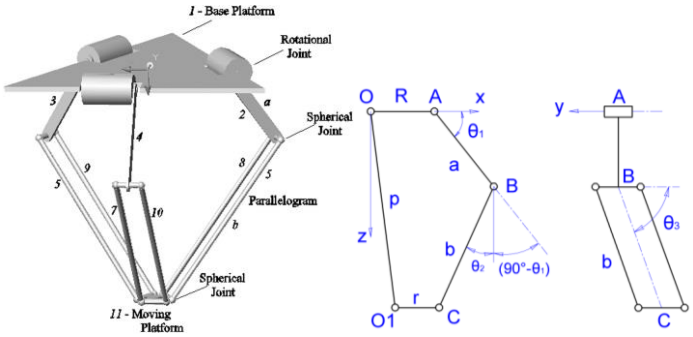

Figure 4. *Design parameters of the delta parallel robot.*

The Delta robot is used here as a case study: it is a lower-pair parallel mechanism whose joint-to-Cartesian transmission is directly characterized by its Jacobian matrix. The central design problem is to choose geometric parameters such that velocity/force transmission is efficient along directions of interest while remaining favorable throughout the entire useful workspace. Traditional indices (nvmin, npmin) capture amplification/attenuation but not the directional nature of transmission that matters in practice — hence GTI's central role in identifying the Pareto frontier over a discrete design domain.

The kinematic analysis of the mechanism corresponding to legs 1, 2, and 3 is derived in this work based on geometric modeling and the fundamental kinematic relations of parallel manipulators, and the resulting equations are given as follows:

$$\begin{vmatrix} p_x \\ p_y \\ p_z \end{vmatrix} + \begin{vmatrix} c\alpha.c\beta & c\alpha.s\beta.s\gamma - s\alpha.c\gamma & c\alpha.s\beta.c\gamma + s\alpha.s\gamma \\ s\alpha.c\beta & s\alpha.s\beta.s\gamma + c\alpha.c\gamma & s\alpha.s\beta.c\gamma - c\alpha.s\gamma \\ -s\beta & c\beta.s\gamma & c\beta.c\gamma \end{vmatrix} . \begin{vmatrix} r \\ 0 \\ 0 \end{vmatrix} - \begin{vmatrix} R \\ 0 \\ 0 \end{vmatrix} = \begin{vmatrix} 0 + b.s_{31} \\ a.c_{11} - b.c_{31}s_{21} \\ a.s_{11} + b.c_{31}.c_{21} \end{vmatrix} \quad (15)$$

$$\begin{vmatrix} p_x \\ p_y \\ p_z \end{vmatrix} + \begin{vmatrix} c\alpha.c\beta & c\alpha.s\beta.s\gamma - s\alpha.c\gamma & c\alpha.s\beta.c\gamma + s\alpha.s\gamma \\ s\alpha.c\beta & s\alpha.s\beta.s\gamma + c\alpha.c\gamma & s\alpha.s\beta.c\gamma - c\alpha.s\gamma \\ -s\beta & c\beta.s\gamma & c\beta.c\gamma \end{vmatrix} . \begin{vmatrix} \frac{-r}{2} \\ \frac{r\sqrt{3}}{2} \\ 0 \end{vmatrix} - \begin{vmatrix} \frac{-R}{2} \\ \frac{R\sqrt{3}}{2} \\ 0 \end{vmatrix} = \begin{vmatrix} 0 + b.s_{32} \\ a.c_{12} - b.c_{32}s_{22} \\ a.s_{12} + b.c_{32}.c_{22} \end{vmatrix} \quad (16)$$

$$\begin{vmatrix} p_x \\ p_y \\ p_z \end{vmatrix} + \begin{vmatrix} c\alpha.c\beta & c\alpha.s\beta.s\gamma - s\alpha.c\gamma & c\alpha.s\beta.c\gamma + s\alpha.s\gamma \\ s\alpha.c\beta & s\alpha.s\beta.s\gamma + c\alpha.c\gamma & s\alpha.s\beta.c\gamma - c\alpha.s\gamma \\ -s\beta & c\beta.s\gamma & c\beta.c\gamma \end{vmatrix} . \begin{vmatrix} \frac{-r}{2} \\ \frac{-r\sqrt{3}}{2} \\ 0 \end{vmatrix} - \begin{vmatrix} \frac{-R}{2} \\ \frac{-R\sqrt{3}}{2} \\ 0 \end{vmatrix} = \begin{vmatrix} 0 + b.s_{33} \\ a.c_{13} - b.c_{33}s_{23} \\ a.s_{13} + b.c_{33}.c_{23} \end{vmatrix} \quad (17)$$

The inverse kinematics problem of the robot is solved numerically using the Generalized Reduced Gradient method [12] and is fully automated through VBA, as illustrated in Figure 5.

Figure 5. *Inverse kinematics solved numerically via the GRG method [12].*

Four design parameters r_1, r_2, r_3, and r_4 in Figure 4, correspond to structural parameters R, r, a, b. Selecting a design surface reduces the unknowns to r_1, r_3, and r_4, since the surface $r_2 = a$ always coincides with the plane $z = 0$, which acts as a constraint surface. The variables are restructured accordingly, as summarized in Table 1.

Table 1. *Assign variables and select initial approximations.*

No.	Original Variable (mm)	Normalized	Initial Approximation (mm)
1	R	r_1	100
2	a	r_3	80
3	b	r_4	155
4	r=R/4		25

Using the constraint surface defined by $r_1 + r_3 + r_4 = 4$, an inward offset of 0.6 mm from the boundary of this surface is introduced to avoid the degeneration of any geometric dimension, as illustrated in Figure 6.

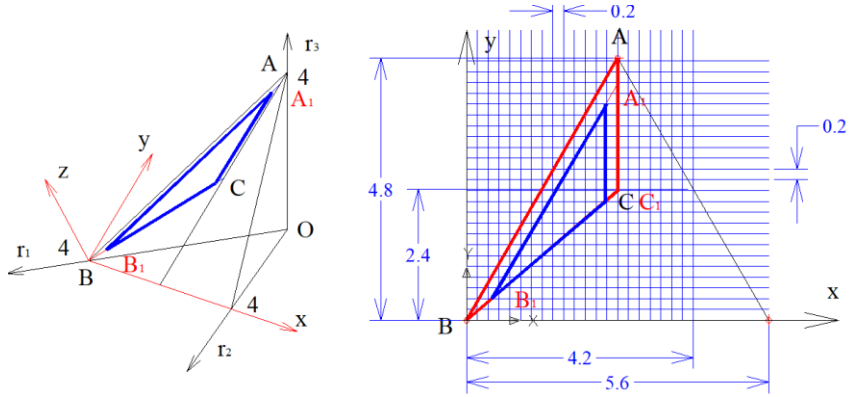

(a) Constraint surface diagram; (b) Grid scheme for the spreading process.

Figure 6. *Design space definition and axis transformation relationship.*

4. RESULTS AND DISCUSSION

The proposed evaluation framework is applied to the Delta parallel robot in order to analyze

the propagation characteristics of transmission indices in the discrete design space. Based on the established design constraints and parameter mapping, the node coordinate scheme used for spectrum spreading is determined as illustrated in Figure 6b.

A partial excerpt of the generated spectrum table is presented in Figure 7, where the design plane is located at $z = 500$. In this study, the GTI index is employed to evaluate both the force transmission coefficient and the velocity transmission coefficient in the discrete design domain.

x	y	z	GTI_npmin	GTI_nvmin	GCI_npmin	GCI_nvmin	Lipschitz npmin	Lipschitz nvmin
80	-100	360	0.004918809	0.415913497	2.0006E-05	0.000535808	0.001308604	0.000997688
100	-100	360	0.021933456	0.818823144	7.99497E-05	0.000997688		
-100	-100	380	0.009792945	0.948940754	1.67601E-05	0.000790992		
-80	-100	380	0.016352646	0.542802812	3.76248E-05	0.000524488		
-60	-100	380	0.000564326	0.250351351	1.53507E-06	0.000263631		
-40	-100	380	0.000256349	0.067836992	7.59641E-07	7.44653E-05		
-20	-100	380	7.14496E-08	0.000289237	2.17047E-10	3.21966E-07		
0	-100	380	0.00013581	0.051679303	4.11605E-07	5.73209E-05		
20	-100	380	3.36553E-06	0.076130587	9.84914E-09	8.31408E-05		
40	-100	380	2.33387E-07	0.001353754	6.52734E-10	1.4433E-06		
60	-100	380	0.000263874	0.142301911	6.94539E-07	0.000147168		

Figure 7. *Numerical atlas of the Delta robot describing GTI, GCI, and Lipschitz performance over the discrete r_i space.*

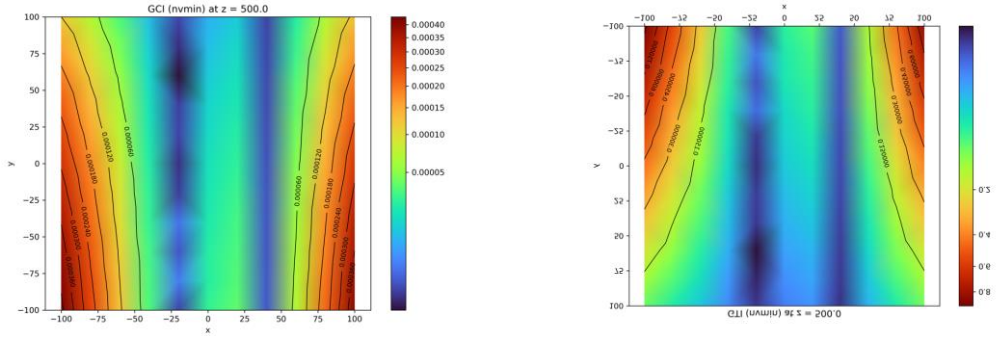

(a) Geometric transmission maps of GCI;

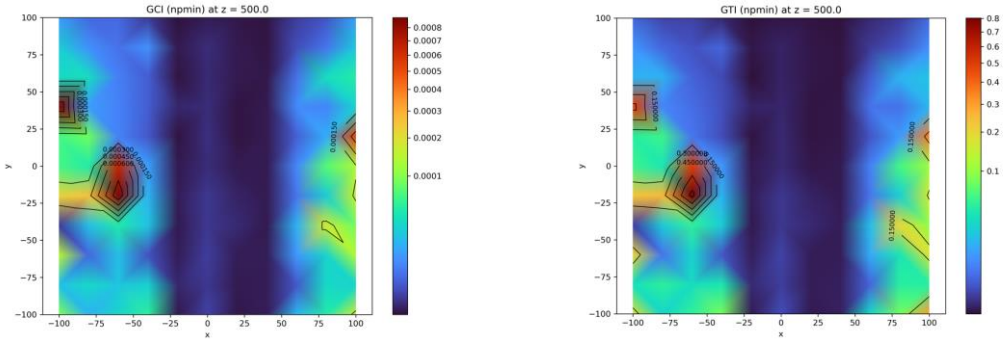

(b) Geometric transmission maps of GTI.

Figure 8. *Geometric transmission maps of GCI and GTI on the plane z = 500.*

In Figure 8, the x and y axes represent the position of the end-effector in the working plane of the robot while the height is fixed at z = 500. The color scale indicates the values of the transmission indices at each point in the workspace, where red–orange colors correspond to higher values, while blue–purple colors correspond to lower values. The contour lines represent iso-value curves, which help visualize the distribution of GTI and GCI over the entire working plane.

In Figure 8, the x and y axes give the end-effector position at fixed height z = 500; red–orange denotes higher index values, blue–purple lower, and contour lines are iso-value curves. The GCI map (8a) describes overall amplification/attenuation; smaller GCI values indicate lower variation and higher stability. Because GCI values are very small throughout, the Delta robot maintains high stability across the considered workspace. The GTI map (8b) instead reveals the formation and variation of directional transmission cones: where the cones associated with npmin or nvmin are well expanded and strongly convergent, GTI is high, indicating strong directional alignment between actuation and end-effector motion.

Based on the spreading results, the coordinates of the optimal point in the dimensionless space, after axis transformation, are obtained as shown in Figure 9:

Reciprocal of rot(x)rot(y)tran(z)

0.714286	-0.40825	0.5873	0
0	0.82222	0.571543	0
-0.71429	-0.40825	0.5873	4
0	0	0	1

Optimal Point

3.4	x
2.6	y
0	z
1	

r

1.4	r3
2.137772	r4
0.509991	r1
1	

Figure 9. *Results of coordinate transformation from the Cartesian workspace to the design space.*

The sum of the coordinates r_1, r_3, and r_4 equals 4, which confirms that the optimal point lies on the constraint surface. By setting L=400, the specific structural parameters of the robot are obtained as follows:

Table 2. *Optimal design results.*

No.	Original Variable (mm)	Normalized	Optimal Value (mm)
1	R	r1	600
2	a	r3	856
3	b	r4	148
4	r = R/4		37

5. CONCLUSIONS

When transitioning to a discrete environment in the design space r_i, the GTI performance indices retain their intuitive directional guidance capability as in the continuous setting; however, they offer a significant advantage in that the identification of the Pareto frontier no longer relies on subjective designer judgment. Recognizing the intrinsic equivalence among the GTI, GCI, and Lipschitz indices reveals that their computation is unified and that they can be flexibly transformed into one another depending on the design requirements.

More importantly, the classical Atlas approach cannot fully automate the design process, whereas the proposed representation of GTI over a discrete domain fundamentally resolves the need for fully automated computation. In essence, the choice among GTI, GCI, and Lipschitz reflects the underlying design philosophy, whether it emphasizes worst-case avoidance (GCI and Lipschitz) or global average optimization (GTI). Given their intrinsic relationships, preparing the GTI alone is sufficient to derive both the GCI and the Lipschitz constant.

Acknowledgement: *This research was supported by the Thai Nguyen University of Technology (TNUT) of Vietnam.*

REFERENCES

[1]. R. Dou. *"Optimum design of 3-RRR planar parallel manipulators"*. Proc. Inst. Mech. Eng. Part C J. Mech. Eng. Sci., vol. 224, no. 2, pp. 411–418, (2010). DOI: 10.1243/09544062JMES1658.

[2]. B. Li, P. Xu, H. Yu, Y. Lou, and X. Yang. *"Design and analysis of parallel robots for a flexible fixturing system with performance atlases"*. IEEE Int. Conf. Intell. Robot. Syst., vol. 2015-Decem, pp. 3152–3157, (2015). DOI: 10.1109/IROS.2015.7353813.

[3]. Q. Meng, X. J. Liu, and F. Xie. *"Design and development of a Schönflies-motion parallel robot with articulated platforms and closed-loop passive limbs"*. Robot. Comput. Integr. Manuf., vol. 77, no. October, (2022). DOI: 10.1016/j.rcim.2022.102352.

[4]. J. Sanjuan et al. *"Methodology for the Design of Parallel Robots Using Performance Atlases: The Case of the Linear Delta Parallel Robot"*. 18th IEEE Int. Multi-Conference Syst. Signals Devices, SSD 2021, pp. 749–754, (2021). DOI: 10.1109/SSD52085.2021.9429507.

[5]. P. Horak and J. Lang. *"Automated Generation of Performance Atlases for Multi-Objective Design Optimization"*. Journal of Mechanical Design, vol. 141, no. 5, Art. no. 051402, (2019).

[6]. L. Mainini and J. R. R. A. Martins. *"Surrogate-Based Optimization Architecture for Design Space Mapping and Pareto Frontier Identification"*. AIAA Journal, vol. 59, no. 2, pp. 642–656, (2021).

[7]. Y. Chen and S. J. Connelly. *"Deep Learning for Automated Synthesis of Performance Maps in Multiobjective Engineering Design"*. Engineering Optimization, vol. 56, no. 3, pp. 412–430, (2024).

[8]. Hung Le Huu, Thuy Le Thi Thu and Long Pham Thanh. *"A Numerical Method of Kinematic Synthesis of Parallel Structures on the Basis of the Maximum Target Optimization Problem"*. ICERA 2024, (2024).

[9]. Hung Le Huu, Thuy Le Thi Thu and Long Pham Thanh. *"Optimal design of Delta parallel robots based on the criteria of firmness dexterity and minimum velocity transmission coefficient"*. ICERA 2024, (2024).

[10]. B. Monsarrat and C. M. Gosselin. *"On the Analysis of the Kinematic and Static Performance of Parallel Mechanisms Using Jacobian Matrices"*. IEEE Transactions on Robotics, vol. 36, no. 4, pp. 1105–1118, (2020).

[11]. X. J. Liu and J. Wang. *"Parallel Manipulators: Kinematics, Dynamics and Control"*. New Jersey, NJ: Wiley-IEEE Press, (2022).

[12]. Thanh Trung Trang, LiWei Guang, Long Thanh Pham, Jian Huang. *"Design and analysis of 3 URS ankle rehabilitation parallel machanism kin-ematics by Generalized Reduced Gradient algorithm"*. Basic & clinical pharmacology & toxicology, (2020).

TÓM TẮT

Đo lường mức độ lan truyền toàn cục và lan truyền có định hướng của một số chỉ số hiệu suất, trong thiết kế tối ưu đa mục tiêu các robot song song, thông qua đánh giá hệ số Lipschitz và hệ số GTI trên miền rời rạc

Trong thiết kế tối ưu đa mục tiêu các robot song song, các chỉ tiêu tỉ suất truyền như n_{vmin}, n_{pmin} được dùng để đánh giá mức độ lan truyền của vận tốc và lực từ không gian khớp (q) sang không gian công tác (x) của robot. Có hai thông tin cần đo lường trong cách đánh giá này là mức độ trùng hướng giữa dẫn động và chấp hành, mức độ khuếch đại/ suy hao của dẫn động khi chuyển thành chấp hành. Để đánh giá các yếu tố này cũng có hai phương pháp là đánh giá mức độ lan truyền trên toàn không gian thông qua hệ số Lipschitz và đánh giá theo một hướng cụ thể được quan tâm thông qua hệ số GTI (Geometric Transmission Index). Trong thuật toán Atlas cải tiến do tác giả phát triển, biên Pareto được định nghĩa là giao thoa của các nón hướng đã hội tụ trên cơ sở các atlas chỉ dẫn lan truyền của các chỉ tiêu thiết kế nói trên. Bài báo này giới thiệu cách đánh giá các hệ số này trên miền thiết kế rời rạc r_i để phục vụ tự động hoá quá trình xác định biên Pareto từ đó làm cơ sở tự động hoá toàn bộ thiết kế.

Từ khóa: Jacobian; GTI; Lan truyền; Lipschitz; Toàn cục.